RSC Advances

PAPER

View Article Online
View Journal | View Issue

Cite this: *RSC Adv.*, 2025, **15**, 5117

Synergistic polyphenol–amino acid nanoparticles: a new strategy for reactive oxygen species management†

Huizhou Ye,‡[a] Jiayin Cai,‡[c] Zhihao Shen,[d] Qiuping Qian [b] and Chunxia Zhang*[a]

Received 2nd December 2024
Accepted 10th February 2025

DOI: 10.1039/d4ra08496a

rsc.li/rsc-advances

Polyphenols exhibit strong antioxidant, and anti-inflammatory but are limited by chemical instability and low bioavailability. To address these challenges, we developed polyphenol–amino acid conjugates that self-assemble into stable nanospheres, enhancing their stability and bioavailability. These nanoparticles demonstrate significantly improved ROS scavenging efficiency and promote cell proliferation *in vitro*. The incorporation of amino acids enhances biocompatibility and facilitates effective ROS elimination. The polyphenol–amino acid nanoparticles offer a multifaceted therapeutic strategy to mitigate oxidative stress, overcoming traditional antioxidant limitations through advanced nanotechnology. This approach contributes to the development of next-generation wound care solutions with enhanced efficacy and safety profiles.

1. Introduction

With the global aging population and the rising incidence of chronic diseases such as diabetes, chronic wounds and hard-to-heal wounds have become urgent medical challenges to be addressed.[1–3] Wound healing is a complex biological process involving multiple stages, including inflammatory response, cell proliferation, and tissue remodeling.[4,5] During this process, reactive oxygen species (ROS) play a dual role: appropriate levels of ROS are crucial for cell signal transduction and immune defense, but excessive ROS can trigger oxidative stress, leading to damage of cell membranes, proteins, and deoxyribonucleic acid (DNA), thereby delaying wound healing.[6–9]

Effective management of ROS levels is therefore pivotal in promoting optimal wound healing. Traditional antioxidant therapies have shown promise.[10–13] However, their clinical application is often limited by factors such as poor stability, low bioavailability, and inadequate targeting to the wound site.[14,15] These limitations underscore the need for innovative delivery systems that can enhance the therapeutic efficacy of antioxidants while minimizing potential side effects. Among the various bioactive compounds explored, polyphenols have garnered significant attention due to their potent antioxidant, anti-inflammatory, and antimicrobial properties.[16–18] Polyphenols, a diverse group of naturally occurring compounds found in plants,[19–22] can effectively scavenge excessive ROS and mitigate oxidative stress, thereby fostering a conducive environment for wound healing.[20] Despite their therapeutic potential, the clinical application of polyphenols is hindered by their inherent limitations, including chemical instability, rapid degradation in biological environments, and limited bioavailability. To overcome these challenges, recent research has focused on developing nanocarrier systems that can encapsulate and protect polyphenols, enhancing their stability and facilitating controlled release at the wound site.[23,24] Amino acid, known for their biocompatibility, versatility, and specific biological functions, have been integrated with polyphenols to form polyphenol–amino acid conjugates.[25,26] These conjugates can self-assemble into nanoparticles, providing a robust platform for delivering antioxidants directly to the wound microenvironment.

Despite the promising prospects, several challenges remain in the development and application of polyphenol–amino acid nanoparticles for wound dressings. These include optimizing the synthesis and characterization of nanoparticles, understanding their interactions with cells, ensuring their biocompatibility and safety, and evaluating their efficacy, addressing these challenges requires a multidisciplinary effort, combining expertise in materials science, chemistry, and biology.

In this study, we developed antioxidant nanoparticles called polyphenol–amino acid nanoparticles by combining tea polyphenols (TP) with arginine (L-Arg, denoted as R) using a self-assembly method. These functional particles can scavenge free radicals and reactive oxygen species, further protecting

[a]*The Second Affiliated Hospital and Yuying Children's Hospital of Wenzhou Medical University, Wenzhou, Zhejiang 325000, China. E-mail: 51774130@qq.com*

[b]*Zhejiang Engineering Research Center for Tissue Repair Materials, Wenzhou Institute, University of Chinese Academy of Sciences, Wenzhou, Zhejiang 325000, China*

[c]*Zhejiang Chinese Medical University, Hangzhou, Zhejiang 310053, China*

[d]*Joint Center of Translational Medicine, The First Affiliated Hospital of Wenzhou Medical University, Wenzhou, Zhejiang 325000, China*

† Electronic supplementary information (ESI) available. See DOI: https://doi.org/10.1039/d4ra08496a

‡ These authors (Huizhou Ye, Jiayin Cai) contributed equally.

connective tissue cells under oxidative stress (Fig. 1). This research will provide a theoretical basis and technical support for developing a new generation of functional wound dressing materials.

2. Experimental section

2.1. Materials

Tea polyphenols, titanium sulfate, titanic sulfate ($Ti(SO_4)_2$) and phosphate-buffered saline (PBS) solution were procured from Shanghai Macklin Biochemical Co., Ltd. 2,2′-Azinobis-(3-ethylbenzthiazoline-6-sulphonate) (ABTS) solution, L-arginine, ferrous sulfate ($FeSO_4$) and polyvinyl alcohol 1788 (PVA) were acquired from Shanghai Aladdin Biochemical Technology Co., Ltd. Additionally, formaldehyde solution (~37%), 3,3′,5,5′-tetramethylbenzidine (TMB), hydrogen peroxide solution, and iron(II) sulfate heptahydrate were purchased from Aldrich. Dulbecco's Modified Eagle Medium (DMEM) and fetal bovine serum (FBS) were kindly provided by Thermo Fisher Scientific. The Cell Counting Kit-8 (CCK-8) was obtained from Beyotime. Furthermore, deionized water (18.2 MΩ cm^{-1}) was sourced from a Milli-Q water purification system. Unless otherwise specified, all other chemicals were utilized without undergoing further purification.

2.2. Synthesis of tea polyphenol@ L-arginine (PTR) nanoparticles

A total of 100 mg of tea polyphenol was dissolved in 50 mL of water at room temperature. To this solution, 200 μL of formaldehyde and varying concentrations of L-arginine were added. Subsequently, 50 mL of a 1% (w/v) polyvinyl alcohol solution was introduced into the mixture. The resulting solution was then subjected to ultrasonication for 2 minutes to ensure homogeneous mixing. Afterward, the solution was stirred at 250 rpm for 24 hours at room temperature to allow for the formation of PTR nanoparticles. Following stirring, the PTR nanoparticles were collected by centrifugation at 8000 rpm for 8 minutes. The collected nanoparticles were subsequently washed three times with deionized water to remove any residual impurities.

2.3. Characterization

Transmission electron microscopy (TEM) images were captured with a JEOL JEM1010 transmission electron microscope operated at an acceleration voltage of 100 kV. The materials were evaluated by Fourier Transform Infrared (FTIR) spectroscopy (Nicolet iS 10). The measurements were carried out at room temperature over the wavenumbers ranging from 500 to 4000 cm^{-1}. The absorbance of the solutions was measured with a Jasco V-730 spectrophotometer. Live/dead cell staining was observed using fluorescence microscopy (Carl Zeiss™ Axio Vert.A1 Inverted Microscope, USA).

2.4. Free radical scavenging test

The free radical scavenging ability of PTR nanoparticles was assessed using 2,2′-azinobis-(3-ethylbenzthiazoline-6-sulphonate). The ABTS radical cation ($ABTS^{+\bullet}$) was generated by incubating 2 mL of ABTS solution (1 mg mL^{-1}) with 2 mL of potassium persulfate solution (1 mg mL^{-1}) overnight at room temperature to allow for complete oxidation. After incubation, 200 μL of the $ABTS^{+\bullet}$ solution was mixed with 1 mL of PTR nanoparticle solution at varying concentrations. The absorbance of the resulting mixture was measured at 734 nm using a UV-vis spectrophotometer to determine the $ABTS^{+\bullet}$ scavenging activity of the nanoparticles.

2.5. Hydrogen peroxide (H_2O_2) scavenging activity assessment

A 10 mM solution of H_2O_2 (0.1 mL) was combined with various concentration of PTR nanoparticles (pH 7.2, PBS) and incubated at intervals: 30 min. Subsequently, 1 mg mL^{-1} of $TiSO_4$ (0.5 mL) was introduced and allowed to react for 5 minutes. The absorbance of the resulting solution (10 mm path length) was measured at 410 nm.

2.6. Hydroxyl radical (·OH) scavenging activity assessment

The scavenging activity of ·OH radicals was evaluated using the TMB chromogenic assay. In this method, ·OH radicals are generated by the classical Fenton reaction between H_2O_2 and $FeSO_4$, which transforms TMB into oxidized TMB (oxTMB)

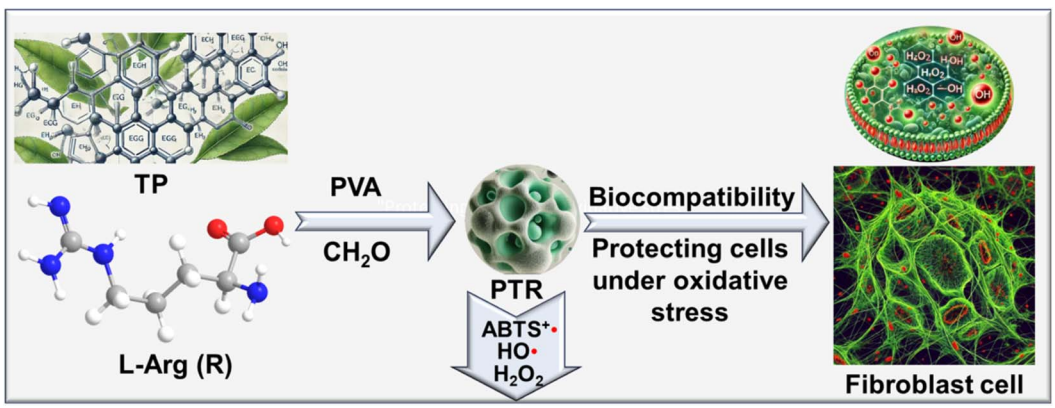

Fig. 1 Process flow for the preparation of polyphenol–amino acid nanoparticles for reactive oxygen species scavenging and cell protection.

exhibiting a characteristic absorbance at 652 nm. Consequently, the concentration of residual ·OH radicals can be quantified by monitoring the absorption at 652 nm. Test solutions were prepared in the dark in PBS buffer (pH = 5.0) containing 1 mM TMB (0. 2 mL), 10 mM H_2O_2 (0.2 mL), 5 mM $FeSO_4$ (0.2 mL) and various concentrations of PTR nanoparticles. The absorbance peak at 652 nm was then monitored using UV-vis spectroscopy.

2.7. Cell culture procedure

L929 cells were cultivated in Dulbecco's Modified Eagle Medium (DMEM) supplemented with 10% fetal bovine serum (Gibco, USA), along with 100 U mL^{-1} of penicillin and 100 μg mL^{-1} of streptomycin. The cells were maintained in an incubator at 37 °C under an atmosphere containing 5% CO_2.

2.8. Cell viability assessment

L929 cells were seeded into 96-well plates at a density of 8×10^3 cells per well. Following the application of various treatments, a working solution of CCK8 (Beyotime, China) was prepared by diluting the CCK8 reagent with serum-free medium at a ratio of 1 : 9, as per the manufacturer's instructions. The cells were then incubated with this working solution in a 37 °C incubator, under dark conditions, for 2 hours. The absorbance of each well was measured using a microplate reader (Varioskan LUX) after incubating for two hours.

2.9. ROS-induced cell viability assessment

L929 cells were seeded into 96-well plates at a density of 8×10^3 cells per well. Once the cells had fully attached, they were treated with H_2O_2 at concentrations of 100 μM and 200 μM to induce reactive oxygen species (ROS) stress. Subsequently, the cells were washed with PBS and treated with PTR NPs (presumably a type of nanoparticle) for 2 hours. Following this treatment, a working solution of CCK8 was prepared according to the manufacturer's instructions and added to the cells. The cells were then incubated with the CCK8 solution in a 37 °C incubator under dark conditions for 2 hours. Finally, the absorbance was measured at a wavelength of 450 nm to assess cell viability under ROS-induced stress conditions.

2.10. Statistical analysis

All the quantitative data were analyzed by the *t*-test, one-way ANOVA with Dunnett's multiple comparison test, or two-way ANOVA with Dunnett's multiple comparison test. The data were presented as mean with s.d. values of $*p < 0.05$, $**p < 0.01$, $***p < 0.001$ and $****p < 0.0001$ were considered statistically significant.

3. Results and discussion

3.1. Synthesis and characterization of the PTR NPs

Regulating the component ratio of arginine to tea polyphenols is a key parameter for successfully constructing PTR nanoparticles. With the assistance of the surfactant PVA as a stabilizer, we successfully synthesized PTR particles of different sizes, as shown in Fig. S1† and 2a–d. Under the condition of [R]/[TP] = 1/2, we obtained spherical particles with relatively smooth surfaces, measuring 146.8 ± 37.67 nm in size. Under the conditions of [R]/[TP] = 1/4 and [R]/[TP] = 1, although nanoparticles could be formed, it was challenging to achieve a high proportion of amino acids in PTR while ensuring particle uniformity and integrity. Pure TP exhibits a negatively biased zeta potential, but after constructing the PTR particles, their negative charge significantly decreased, indirectly indicating the successful formation of PTR nanoparticles (Fig. 2e). We further evaluated the nanoparticles using infrared spectroscopy, which confirmed the corresponding characteristics of arginine and tea polyphenols. Specifically, the nanoparticles display a broad absorption band at 3200–3550 cm^{-1} due to overlapping O–H and N–H stretching vibrations from phenolic hydroxyl and amino groups. The aromatic C=C stretching vibrations appear at 1500–1600 cm^{-1}, and C–O stretching vibrations are observed at 1200–1300 cm^{-1}, indicating the phenolic structures of tea polyphenols. For arginine, a strong absorption band at 1700–1750 cm^{-1} corresponds to the C=O stretching vibrations of carboxyl groups, while peaks at 1600–1650 cm^{-1} are attributed to N–H bending and C=N stretching vibrations of the guanidino group unique to arginine (Fig. 2f and S2†). These combined spectral features confirm the presence of both tea polyphenols and arginine in the nanoparticles.

3.2. Free radical scavenging capacity of the PTR NPs

To evaluate the antioxidant capacity of the synthesized PTR nanoparticles (PTR NPs), free radical scavenging experiments were conducted using ABTS.[27,28] The cationic radical $ABTS^{+\bullet}$ appears blue-green but reverts back to colorless ABTS in the presence of antioxidants, accompanied by a decrease in the absorption peak at approximately 738 nm. After mixing $ABTS^{+\bullet}$ with PTR NPs, the color of the solution gradually lightened from blue-green to almost colorless as the concentration of PTR NPs increased. Simultaneously, the characteristic absorption peak of $ABTS^{+\bullet}$ at ~738 nm gradually decreased (Fig. 3a and b).

3.3. Reactive oxygen species scavenging capacity of the PTR NPs

As the concentration of PTR NPs increased, the corresponding absorbance decreased. When the concentration reached 125 μg mL^{-1}, the corresponding absorbance was nearly zero, indicating their superior ROS scavenging ability (Fig. 3c). Moreover, hydroxyl radicals (·OH) are the most destructive reactive oxygen species (ROS) because they can degrade DNA and cell membranes.[29,30] To further investigate the antioxidant properties of PTR nanoparticles, we used additional probes. When TMB is mixed with hydrogen peroxide and ferrous ions, it produces a blue-colored TMB + ·OH complex.[29] In the presence of antioxidants, TMB + ·OH is reduced back to colorless TMB, accompanied by a reduction in the characteristic absorption peak at approximately 652 nm (Fig. S3†). As shown in Fig. 4a, as the concentration of PTR NPs increased, the corresponding absorbance decreased, and ·OH scavenging reached over 90% at 125 μg mL^{-1} (Fig. 4a). These results indicate that PTR NPs have a powerful scavenging effect on ·OH radicals. In addition,

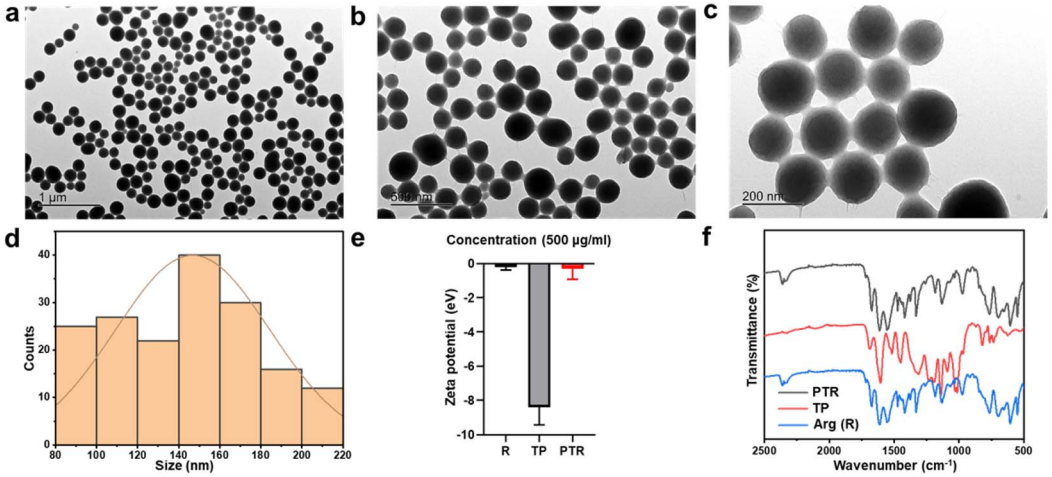

Fig. 2 Nanoparticle size and surface characteristics: TEM images of PTR nanoparticles at low, medium, and high magnifications, (a) scale bar: 1 μm, (b) scale bar: 500 nm, (c) scale bar: 200 nm. (d) Particle size distribution chart of PTR NPs, $d = 146.8 \pm 37.67$ nm. (e) Zeta potential of PTR NPs. (f) FTIR spectrum of PTR NP, TP, Arg (R).

the hydroxyl radical scavenging ability of PTR nanoparticles was further analyzed, using arginine (Arg), tea polyphenols (TP), and ascorbic acid (AA) as positive controls. PTR NPs exhibited a more pronounced ·OH scavenging ability than ARG, and their effectiveness was comparable to that of AA at the same dosage. This indicates that PTR NPs have a strong potential for neutralizing ·OH radicals, matching the efficiency of AA under equivalent conditions (Fig. 4c and S4†).

Hydrogen peroxide (H_2O_2) is a strong oxidizing agent capable of generating reactive oxygen species.[31,32] These ROS can attack lipids, proteins, and DNA in skin cells, leading to cell membrane damage, protein denaturation, and genetic material harm, which may ultimately result in cell death.[33,34] Therefore, we examined the scavenging efficiency of PTR nanoparticles on H_2O_2 by detecting the characteristic absorption peak at 410 nm produced by the reaction of $Ti(SO_4)_2$ with H_2O_2.

As shown in Fig. 4b, the results demonstrated that PTR NPs exhibited a potent scavenging effect on H_2O_2, and this effect was further enhanced with increasing concentrations of PTR NPs. Specifically, within 5 minutes, PTR NPs were able to scavenge 30% of the hydrogen peroxide, indicating their good antioxidant capacity. In addition, we measured the antioxidant properties of PTR using a hydrogen peroxide probe under the same concentration gradient. Arginine, tea polyphenols, and ascorbic

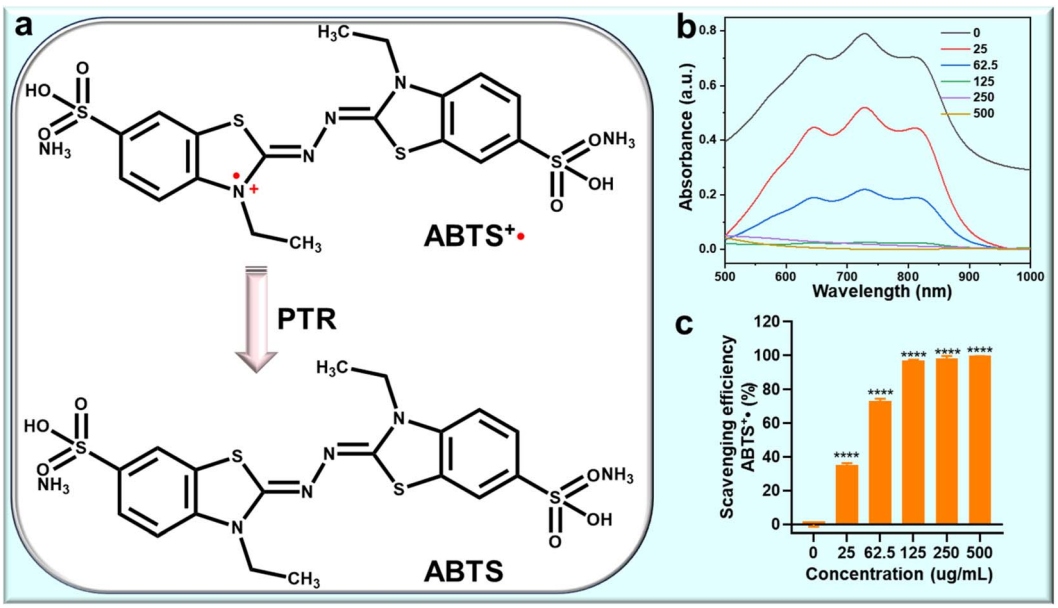

Fig. 3 Free radical scavenging $ABTS^{+\bullet}$ assays of PTR NPs: (a) a schematic illustration depicting the $ABTS^{+\bullet}$ radical scavenging process. (b) UV-vis spectra of $ABTS^{+\bullet}$ radicals after incubation with varying concentration gradients of PTR NPs. (c) Quantitative analysis of $ABTS^{+\bullet}$ radical scavenging effects of PTR NPs at different concentrations.

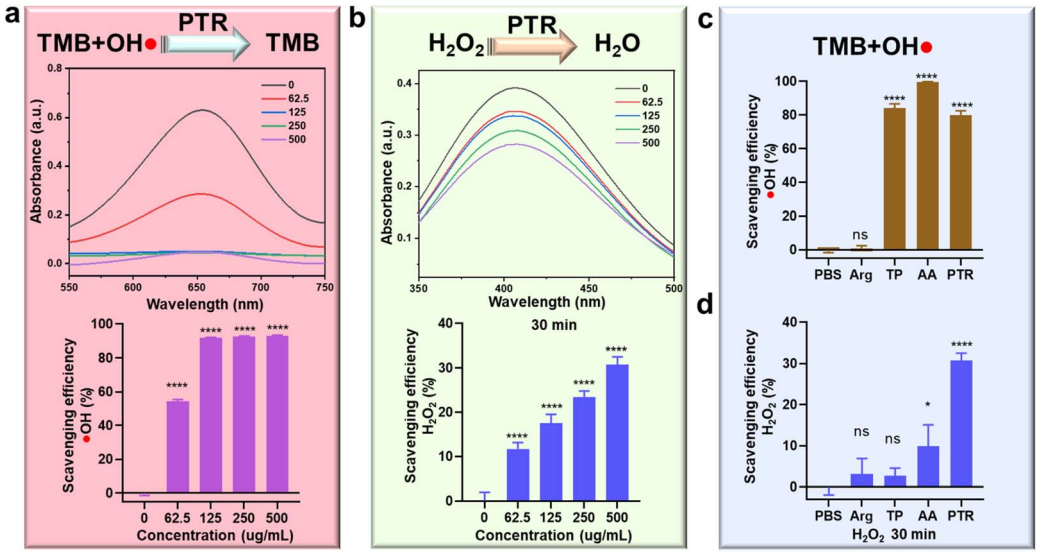

Fig. 4 Reactive oxygen species (ROS) scavenging HO· and H_2O_2 assays of PTR NPs: (a) UV-vis absorbance spectra of TMB + OH· after incubation with varying concentration gradients of PTR NPs, TMB + OH· scavenging activity of PTR NPs at different concentration gradients. (b) UV-vis absorbance spectra of H_2O_2–$Ti(SO_4)_2$ after incubation with varying concentration gradients of PTR NP, H_2O_2–$Ti(SO_4)_2$, scavenging activity of PTR NPs at different concentration gradients. (c)TMB + OH· scavenging effects of Arg, TP, AA, and PTR NPs with 500 μg mL^{-1}. (d) H_2O_2–$Ti(SO_4)_2$ scavenging effects of Arg, TP, AA, and PTR NPs with 500 μg mL^{-1}.

acid a recognized antioxidant, were used as positive controls. The free radical scavenging effect of PTR NP was much stronger than that of ARG, TP, and AA (Fig. 4d). All these results indicate that PTR nanoparticles (PTR NPs) possess superior free radical scavenging ability, making them promising for the treatment of ROS-related skin oxidative stress diseases.

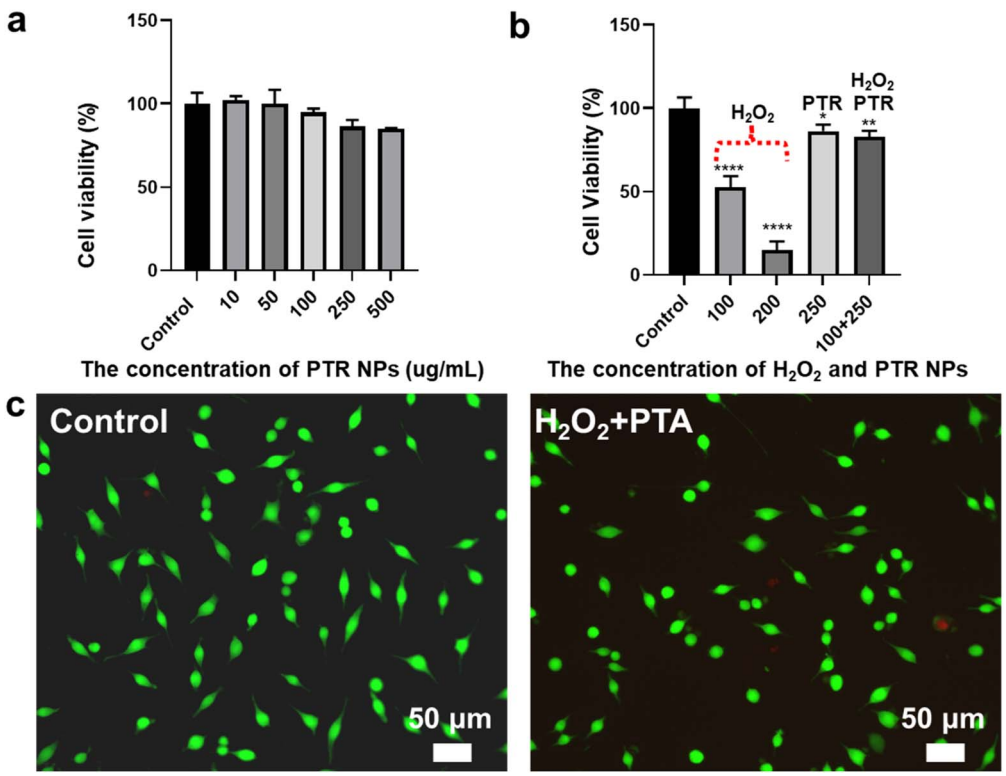

Fig. 5 Cytotoxicity and cell viability under oxidative stress: (a) cell viability of L929 cells by treatment with different concentrations of PTR NPs. (b) Cell viability of L929 cells in different treatment conditions. (c) Fluorescence microscopy images of a live/dead assay of L929 cells, L929 cells were cultured for 2 hours under standard conditions and co-cultured with PTR and H_2O_2. Live cells are stained green, while dead cells are stained red scale bar: 50 μm.

3.4. Biocompatibility of PTR NPs and inhibition of cell death by scavenging ROS

Furthermore, biocompatibility is an essential requirement for functional nanoparticles as dressing materials. Therefore, CCK8 assays were performed to assess the cytocompatibility of PTR nanoparticles (PTR NPs).[35] Fibroblasts (L929) were co-cultured and cell viability was evaluated using the CCK8 assay (Fig. 5a). Treatment with PTR nanoparticles (PTR NPs) for 2 hours at 250 μg mL^{-1} resulted in approximately 90% cell survival, while increasing the concentration to 500 μg mL^{-1} maintained survival rates above 85%, indicating minimal toxicity to normal connective tissue cells. To examine the protective mechanism of PTR, L929 cells were exposed to 100 μM hydrogen peroxide (H_2O_2) to induce oxidative stress and subsequently treated with PTR NPs. Cell survival rates in PTR-treated groups exceeded 85%, significantly higher than those treated with H_2O_2 alone, demonstrating the antioxidant efficacy of PTR NPs in mitigating oxidative stress in mammalian cells (Fig. 5b). Cell viability was further evaluated using live/dead fluorescence staining. As shown in Fig. 5c, most fibroblasts treated with PTR NPs and H_2O_2 were viable, as evidenced by positive staining with calcein-AM and green fluorescence. In contrast, few dead cells were stained by propidium iodide (PI), showing red fluorescence. These results indicate that the polyphenol peptide nanoparticles can scavenge reactive oxygen species, thereby protecting cells.

4. Conclusion

In this study, we synthesized poly(tea polyphenol)-arginine nanoparticles (PTR NPs) and evaluated their antioxidant properties and biocompatibility for treating reactive oxygen species (ROS)-related skin oxidative stress diseases. PTR NPs demonstrated superior free radical scavenging abilities compared to arginine, tea polyphenols, and ascorbic acid, effectively scavenging 30% of hydrogen peroxide within 5 minutes and over 90% of hydroxyl radicals at 125 μg mL^{-1}. Biocompatibility assessments using L929 fibroblast cells showed minimal cytotoxicity, with cell viability remaining above 85% even at concentrations up to 500 μg mL^{-1}. PTR NPs also protected cells from H_2O_2-induced oxidative stress, maintaining high survival rates. These findings indicate that PTR NPs possess strong antioxidant capabilities and excellent biocompatibility, making them promising candidates for treating skin oxidative stress conditions.

Data availability

All data supporting the findings of this study are included within the article and its ESI files.†

Author contributions

Huizhou Ye: investigation, writing – review & editing. Jiayin Cai: investigation, validation, writing – original draft. Zhihao Shen: investigation, methodology, writing – review & editing. Qiuping Qian: writing – original draft, funding acquisition, validation, resources, conceptualization, supervision. Chunxia Zhang: resources, writing – original draft.

Conflicts of interest

There are no conflicts to declare.

Acknowledgements

Qiuping Qian was supported by Major Science and Technology Project of Wenzhou Science and Technology (ZG2022017).

References

1 H. Sun, L. Pulakat and D. W. Anderson, *Curr. Drug Targets*, 2020, **21**, 1264–1275.
2 C. K. Sen, *Adv. Wound Care*, 2019, **8**, 39–48.
3 M. Farahani and A. Shafiee, *Adv. Healthcare Mater.*, 2021, **10**, 2100477.
4 A. Hassanshahi, M. Moradzad, S. Ghalamkari, M. Fadaei, A. J. Cowin and M. Hassanshahi, *Cells*, 2022, **11**, 2953.
5 A. Hassanshahi, M. Moradzad, S. Ghalamkari, M. Fadaei, A. J. Cowin and M. Hassanshahi, *Cells*, 2022, **11**, 2953.
6 L. Deng, C. Du, P. Song, T. Chen, S. Rui, D. G. Armstrong and W. Deng, *Oxid. Med. Cell. Longev.*, 2021, **2021**, 8852759.
7 S. Polaka, P. Katare, B. Pawar, N. Vasdev, T. Gupta, K. Rajpoot, P. Sengupta and R. K. Tekade, *ACS Omega*, 2022, **7**, 30657–30672.
8 X. He, J. Xue, L. Shi, Y. Kong, Q. Zhan, Y. Sun, Q. Zhang, S. Ramakrishna and Y. Dai, *Mater. Today Nano*, 2022, **17**, 100149.
9 C. Tu, H. Lu, T. Zhou, W. Zhang, L. Deng, W. Cao, Z. Yang, Z. Wang, X. Wu and J. Ding, *Biomaterials*, 2022, **286**, 121597.
10 H. J. Forman and H. Zhang, *Nat. Rev. Drug Discovery*, 2021, **20**, 689–709.
11 S. Alfei, G. C. Schito, A. M. Schito and G. Zuccari, *Int. J. Mol. Sci.*, 2024, **25**, 7182.
12 W. Fu, S. Sun, Y. Cheng, J. Ma, Y. Hu, Z. Yang, H. Yao and Z. Zhang, *Chem. Eng. J.*, 2024, 153640.
13 C. Zhang, X. Wang, J. Du, Z. Gu and Y. Zhao, *Advanced Science*, 2021, **8**, 2002797.
14 S. Sharifi, M. J. Hajipour, L. Gould and M. Mahmoudi, *Mol. Pharm.*, 2020, **18**, 550–575.
15 J. Chen, Q. Zhou and W. Cao, *Adv. Funct. Mater.*, 2024, **34**, 2405844.
16 B. Hu, Y. Ouyang, T. Zhao, Z. Wang, Q. Yan, Q. Qian, W. Wang and S. Wang, *Adv. Healthcare Mater.*, 2024, **13**, 2303817.
17 M. Sobhani, M. H. Farzaei, S. Kiani and R. Khodarahmi, *Food Rev. Int.*, 2021, **37**, 759–811.
18 N. K. Bhol, M. M. Bhanjadeo, A. K. Singh, U. C. Dash, R. R. Ojha, S. Majhi, A. K. Duttaroy and A. B. Jena, *Biomed. Pharmacother.*, 2024, **178**, 117177.
19 U. Ghani, in *Alpha-Glucosidase Inhibitors*, ed. U. Ghani, Elsevier, 2020, pp. 61–100.

20 M. Krawczyk, I. Burzynska-Pedziwiatr, L. A. Wozniak and M. Bukowiecka-Matusiak, *Biomolecules*, 2023, **13**, 1402.
21 A. Belščak-Cvitanović, K. Durgo, A. Huđek, V. Bačun-Družina and D. Komes, in *Polyphenols: Properties, Recovery, and Applications*, ed. C. M. Galanakis, Woodhead Publishing, 2018, pp. 3–44.
22 K. B. Pandey and S. I. Rizvi, *Oxid. Med. Cell. Longev.*, 2009, **2**, 270–278.
23 Y. Guo, Q. Sun, F. Wu, Y. Dai and X. Chen, *Adv. Mater.*, 2021, **33**, 2007356.
24 Z. Chen, M. A. Farag, Z. Zhong, C. Zhang, Y. Yang, S. Wang and Y. Wang, *Adv. Drug Deliv. Rev.*, 2021, **176**, 113870.
25 T. Wang, C. Ménard-Moyon and A. Bianco, *Chem. Soc. Rev.*, 2022, **51**, 3535–3560.
26 Z. Yi, G. Chen, X. Chen, Z. Sun, X. Ma, W. Su, Z. Deng, L. Ma, Y. Ran, Q. Tong and X. Li, *ACS Sustainable Chem. Eng.*, 2020, **8**, 9833–9845.
27 X. Li, Z. Han, T. Wang, C. Ma, H. Li, H. Lei, Y. Yang, Y. Wang, Z. Pei, Z. Liu, L. Cheng and G. Chen, *Biomaterials*, 2022, **291**, 121904.
28 Q. Chen, Q. Qian, H. Xu, H. Zhou, L. Chen, N. Shao, K. Zhang, T. Chen, H. Tian, Z. Zhang, M. Jones, K. Y. H. Kwan, M. Sewell, S. Shen, X. Wang, M. A. Khan, P. Makvandi, S. Jin, Y. Zhou and A. Wu, *ACS Nano*, 2024, **18**, 8885–8905.
29 K. Jomova, R. Raptova, S. Y. Alomar, S. H. Alwasel, E. Nepovimova, K. Kuca and M. Valko, *Arch. Toxicol.*, 2023, **97**, 2499–2574.
30 Z. Wang, P. Zhang, C. Yin, Y. Li, Z. Liao, C. Yang, H. Liu, W. Wang, C. Fan and D. Sun, *Adv. Funct. Mater.*, 2023, **33**, 2300341.
31 J. Bäckvall, *Modern Oxidation Methods*, 2004, pp. 193–222.
32 S. S. Acharyya, S. Ghosh, S. Adak, T. Sasaki and R. Bal, *Catal. Sci. Technol.*, 2014, **4**, 4232–4241.
33 S. Gao, C. Qu, J. Wang, K. Qian and Z. Cheng, *Nano Today*, 2024, **59**, 102478.
34 A. S. Tolmacheva and G. A. Nevinsky, *Int. J. Mol. Sci.*, 2022, **23**, 3898.
35 J. Zhu, A. Wang, X. Miao, H. Ye, S. Pan, C. Zhang, Q. Qian and F. Su, *RSC Adv.*, 2023, **13**, 30453–30461.